

Supporting Information (SI)

Fe(100)-(Borazine)_{n=1 to 4}-Fe(100): A multifunctional spin diode with spin valve action

Sayantanu Koley^a, Sabyasachi Sen^b, Snehasish Saha^b, Swapan Chakrabarti^a

^a *Department of Chemistry, University of Calcutta
92, A.P.C.Ray Road, Kolkata 700 009*

India

email: swapanchem@yahoo.co.in

^b *Department of Physics, JIS College of Engineering,
Block-A, Phase-III, Kalyani, Nadia, PIN- 741235*

India

email: sabyaphy12@gmail.com

Content of SI:

Coordinates of the optimized geometry of (borazine)_{n=1to4} [(B₃N₃H₆)_{n=1to4}]- thiol ended

Figure S1. (a) Current voltage characteristic (b) spin polarized rectification ratio, of Fe(100)-(borazine)_{n=2}-Fe(100) under AFM arrangement of electrodes.

Figure S2. (a) Current voltage characteristic (b) spin polarized rectification ratio, of Fe(100)-(borazine)_{n=3}-Fe(100) under AFM arrangement of electrodes.

Figure S3. (a) Current voltage characteristic (b) spin polarized rectification ratio, of Fe(100)-(borazine)_{n=4}-Fe(100) under AFM arrangement of electrodes.

Figure S4. MPSH states corresponding to the SOHMO of the (a) Fe (100)- (borazine)_{n=1} - Fe(100) system obtained at -1V for spin up (b) Fe (100)- (borazine)_{n=2} -Fe(100) system obtained at -1V for spin down (c) Fe (100)- (borazine)_{n=2} -Fe(100) system obtained at 1V for spin up (d) Fe (100)- (borazine)_{n=2} -Fe(100) system obtained at +1V for spin down (e) Fe (100)- (borazine)_{n=3} -Fe(100) system obtained at -1V for spin up (f) Fe (100)- (borazine)_{n=4} -Fe(100) system obtained at -1V for spin down, (g) Fe (100)- (borazine)_{n=4} -Fe(100) system obtained at +1V for spin up (d) Fe (100)- (borazine)_{n=4} - Fe(100) system obtained at +1V for spin down.

Figure S5. Current (I)- voltage (V) characteristic of (a) Fe(100)-borazine-Fe(100), (b) Fe(100)-(borazine)₂-Fe(100), (c) Fe(100)-(borazine)₃-Fe(100), (d) Fe(100)-(borazine)₄-Fe(100); under FM arrangement of electrodes.

Figure S6: Bias dependence of the net current ($I_{\text{spin up}} + I_{\text{spin down}}$) obtained with spin parallel (FM) and spin anti-parallel (AFM) arrangements of Fe (100) electrodes in case of (a) Fe(100)-borazine -Fe(100), (b) Fe(100)-(borazine)₂-Fe(100), (c) Fe(100)-(borazine)₃-Fe(100) and (d) Fe(100)-(borazine)₄-Fe(100).

Figure S7. Bias dependence of the TMR of (a) Fe(100)-(borazine)₂-Fe(100), (b) Fe(100)-(borazine)₃-Fe(100) and (c) Fe(100)-(borazine)₄-Fe(100).

Figure S8. Current voltage characteristic of Fe(100)- (borazine)_{n=1}-Fe(100) having the electrodes with spin anti-parallel (AFM) arrangements under variable gate field using two different dielectrics (a) SiO₂ (b) HfO₂

Figure S9: (a) Energy levels of borazine before and after the image potential correction, (b) PDOS of borazine, (c) Partial density of states of Fe 3d electrons.

Figure S10. Projected device density of states of 'p' orbitals of sulfur of Fe(100)-borazine-Fe(100) under (a) AFM and (b) FM arrangement of electrodes at -1V potential and (c) AFM and (d) FM arrangement of electrodes at 1V potential.

Coordinates of the optimized geometry of borazine (B₃N₃H₆)-thiol ended

H	-1.32591068	2.42710250	0.07255537
H	-1.47160549	-2.18553209	-0.18410799
H	1.07709962	-2.04788343	-0.07430288
H	1.20853123	2.11813175	0.15750271
B	1.40753200	0.02629116	0.05174694
B	-0.82260277	-1.19629184	-0.10426268
B	-0.74075596	1.39629751	0.03999648
N	0.57397895	-1.16900491	-0.04671172
N	-1.51407948	0.12469006	-0.06019368
N	0.65105880	1.27504624	0.08927922
S	3.17769509	-0.03287308	0.11959487
S	-3.15781467	0.18002352	-0.12317433

Coordinates of the optimized geometry of (borazine)₂ [(B₃N₃H₆)₂]- thiol ended

N	0.72708400	0.00240400	0.00085700
N	2.89639800	-1.20257400	0.14691700
H	0.92590200	2.28179800	-0.28370200
H	0.92548800	-2.27739600	0.28585200
H	3.37548100	2.08926400	-0.25907500
B	1.47224900	-1.22737400	0.14884700
B	1.47138200	1.23084500	-0.14686900
B	3.65154500	0.00270700	0.00102100
N	2.89743600	1.20858000	-0.14481800
H	3.38042900	-2.08094700	0.26046100
N	-3.64756300	-0.00045400	0.00160600
N	-1.51485100	-1.20169900	-0.15545700
H	-3.52427000	2.27430800	0.27863700
H	-3.52073100	-2.27049900	-0.31108100
H	-1.02783900	2.07940600	0.26816700
B	-2.93741200	-1.24484400	-0.16769900
B	-2.93933800	1.24730400	0.15208500
B	-0.74680900	0.00188600	-0.00038500
N	-1.51663700	1.20489800	0.15160900
H	-1.02445400	-2.07448000	-0.27837000
S	-5.38972600	0.00789800	-0.07416500
S	5.49302600	-0.08435800	0.01104500

Coordinates of the optimized geometry of (borazine)₃ [(B₃N₃H₆)₃]- thiol ended

H	5.72796800	-2.28818700	0.10152000
H	5.72466400	2.28832600	-0.13713000
H	3.22761200	2.09018100	-0.11813100
H	3.23054900	-2.09253600	0.10346400
B	2.94825800	-0.00105800	-0.00178200
B	5.14038700	1.25481300	-0.07307100
B	5.14217800	-1.25458800	0.05463600
N	3.71882900	1.21092000	-0.06440600
N	5.85143900	0.00110700	0.00068300
N	3.72051900	-1.21216600	0.05712600
H	1.27021400	-2.27158000	-0.35138700
H	1.26972100	2.26767800	0.35291000
H	-1.17949700	2.06640600	0.32207500
H	-1.17862100	-2.07124400	-0.31896100
B	-1.47081400	-0.00234900	0.00178800
B	0.72537800	1.21962100	0.18330100
B	0.72579200	-1.22354800	-0.18157500
N	-0.69615300	1.19294900	0.17937000
N	1.47735500	-0.00181600	0.00027800
N	-0.69581100	-1.19759700	-0.17583200
H	-3.14078300	-2.28841000	0.22593000
H	-3.13967100	2.28440900	-0.22195800
H	-5.59566600	2.08761300	-0.20331500
H	-5.59142200	-2.09499900	0.20607600
B	-5.86681200	-0.00217500	0.00104800
B	-3.68761000	1.23170300	-0.11349900
B	-3.68717500	-1.23466300	0.11712600
N	-5.11136800	1.20670800	-0.11253100
N	-2.94288100	-0.00231000	0.00197200
N	-5.11285300	-1.21181600	0.11557700
S	-7.70780000	0.08561600	-0.00761300
S	7.59297900	-0.00133400	-0.07213500

Coordinates of the optimized geometry of (borazine)₄ [(B₃N₃H₆)₄]- thiol ended

H	7.93564400	2.30670200	0.02460900
H	7.93567700	-2.30666600	-0.02522800
H	5.42566300	-2.09778600	-0.02277100
H	5.42563200	2.09777700	0.02297700
B	5.14611400	-0.00000600	0.00012600
B	7.33331300	-1.28397300	-0.01411500
B	7.33329500	1.28400000	0.01368400
N	5.92827600	-1.22026900	-0.01324700
N	8.07034400	0.00002000	-0.00034700
N	5.92825800	1.22027000	0.01328700
S	9.73519900	0.00003600	-0.00064900
H	3.48263100	2.30339300	0.02766900
H	3.48265100	-2.30342900	-0.02691500
H	1.03196800	-2.09460800	-0.02398900
H	1.03195100	2.09455000	0.02489000
B	0.73458700	-0.00003000	0.00042900
B	2.93316200	-1.24072800	-0.01423400
B	2.93315200	1.24068700	0.01497900
N	1.52037300	-1.21043500	-0.01362700
N	3.69552300	-0.00001600	0.00030800
N	1.52036300	1.21038100	0.01449400
H	-0.93420800	2.30130300	0.04673500
H	-0.93423400	-2.30135900	-0.04595400
H	-3.38545200	-2.09405400	-0.04184800
H	-3.38543300	2.09402800	0.04232900
B	-3.68277200	-0.00001100	0.00020900
B	-1.48275900	-1.23742200	-0.02372300
B	-1.48274700	1.23737500	0.02441000
N	-2.89830800	-1.20959200	-0.02300000
N	-0.72328400	-0.00002700	0.00038800
N	-2.89829700	1.20955900	0.02354500
H	-5.35116300	2.30121900	-0.09436900
H	-5.35121900	-2.30121300	0.09450900
H	-7.80653400	-2.09702800	0.09584000
H	-7.80648100	2.09706600	-0.09635500
B	-8.09739200	0.00002100	-0.00030500
B	-5.89975300	-1.23774800	0.04953200
B	-5.89972400	1.23776100	-0.04954400
N	-7.31649100	-1.21487900	0.05238700
N	-5.14336700	0.00000100	0.00007500
N	-7.31646200	1.21491000	-0.05276900
S	-9.90444700	0.00002800	-0.00059000

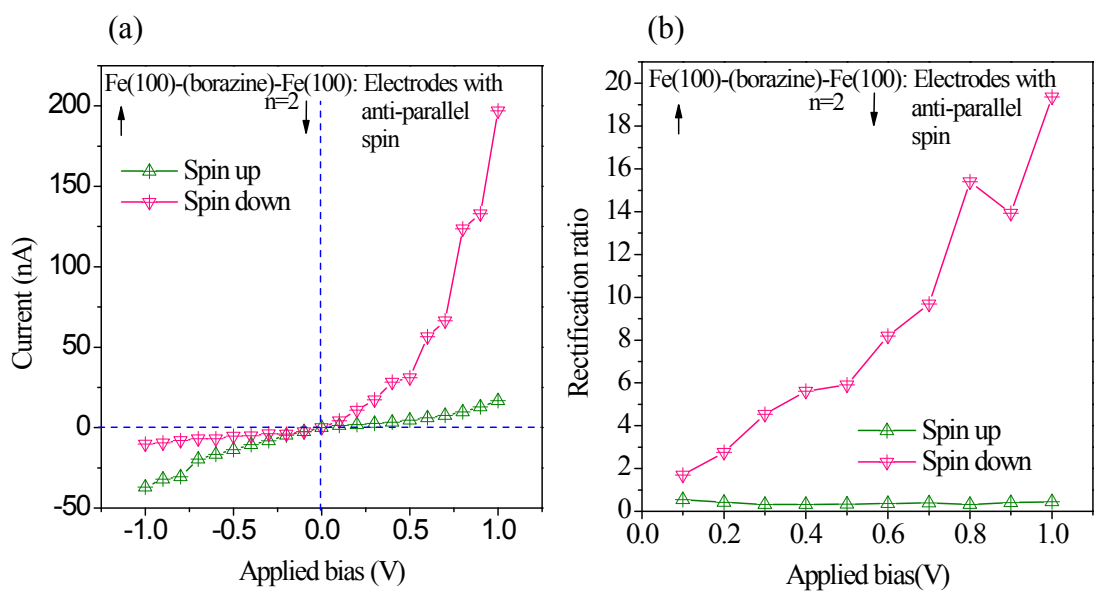


Figure S1. (a) Current voltage characteristic (b) spin polarized rectification ratio, of Fe(100)-(borazine)_{n=2}-Fe(100) under AFM arrangement of electrodes.

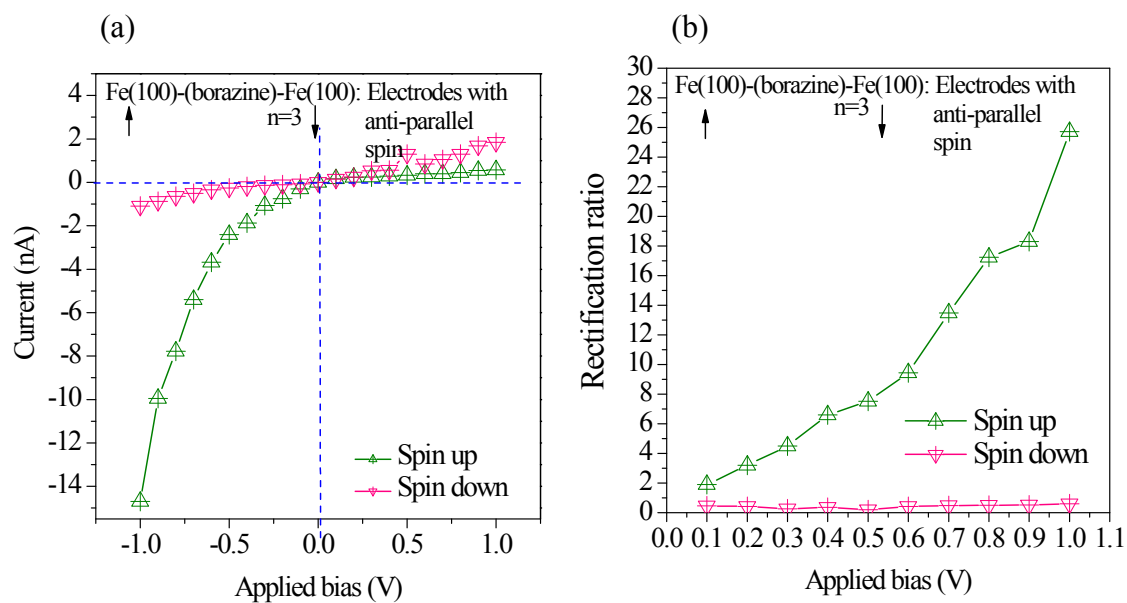


Figure S2. (a) Current voltage characteristic (b) spin polarized rectification ratio, of Fe(100)-(borazine)_{n=3}-Fe(100) under AFM arrangement of electrodes.

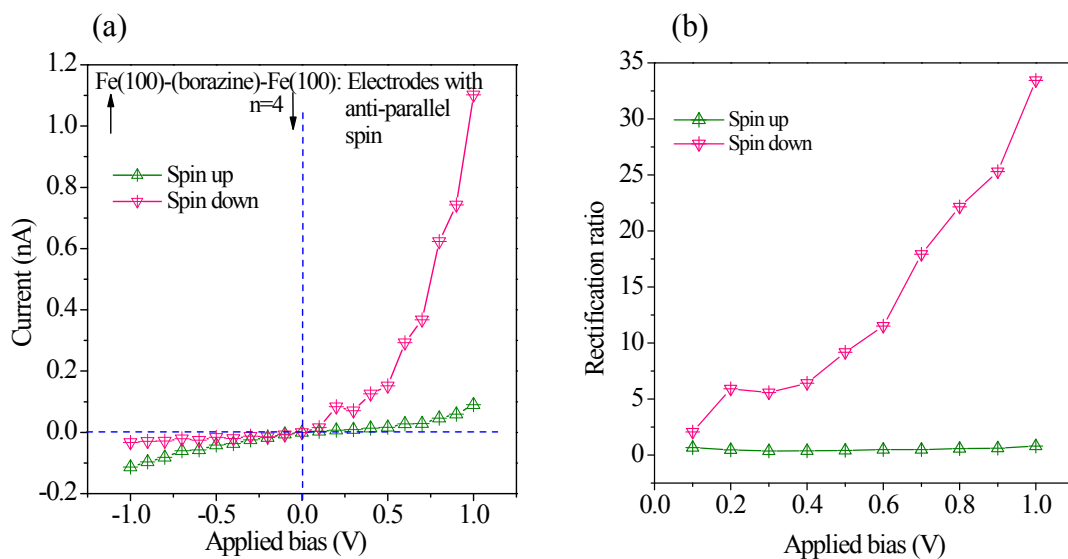


Figure S3. (a) Current voltage characteristic (b) spin polarized rectification ratio, of Fe(100)-(borazine)_{n=4}-Fe(100) under AFM arrangement of electrodes.

Discussion on rectification: In order to see the effect of oligomeric chain length of borazine, we have considered maximum up to tetramer since beyond this limit the current obtained from the two-probe set up is marginal. The figures S1, S2 and S3 represent the I-V characteristics along with the relevant rectification ratio of the di-, tri- and tetramer unit obtained from the anti-parallel spin orientation of the Fe(100) electrodes. The figures clearly reveal that the current rectification comes from the spin down channel for even number of borazine unit while the same rectifier behavior is observed in the spin up channel for the trimer and consistent with the monomer unit. This even-odd phenomenon with respect to spin resolved current rectification is quite unique. This interesting feature can be explained by analyzing the relevant MPSH states as depicted in Fig. S4. It is clearly evident that while the spin up SOHMOs are more delocalized for odd units, the SOHMOs are delocalized in the spin down channel which ultimately is responsible for even-odd behavior in the net spin resolved rectification. Furthermore, it has also been observed that the current rectification gradually increases with the increase in oligomeric chain length though the current obtained from both the spin channel decreases due to enhancement of the tunnel barrier.

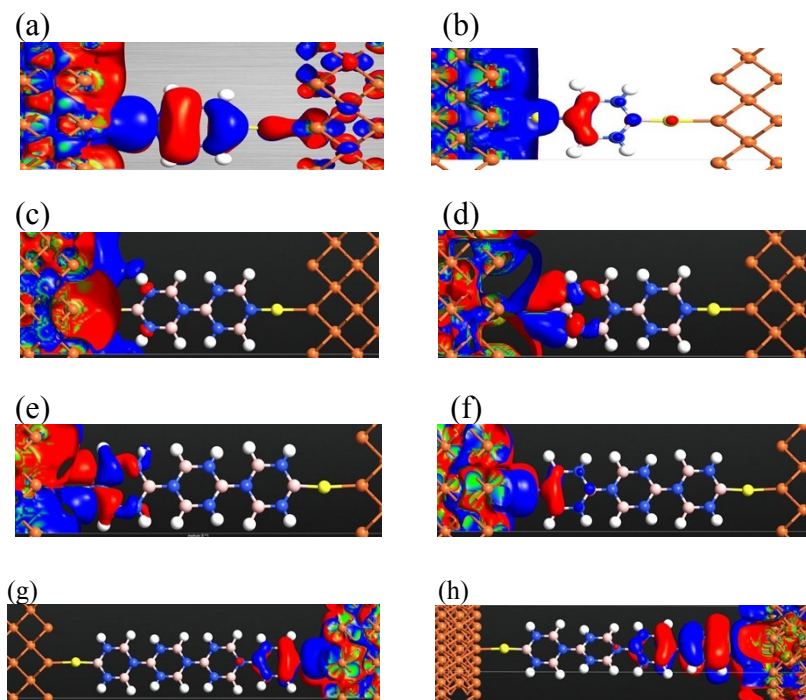


Figure S4. MPSH states corresponding to the SOHMO of the (a) Fe (100)- (borazine)_{n=1} - Fe(100) system obtained at -1V for spin up (b) Fe (100)- (borazine)_{n=2} -Fe(100) system obtained at -1V for spin down (c) Fe (100)- (borazine)_{n=2} -Fe(100) system obtained at 1V for spin up (d) Fe (100)- (borazine)_{n=2} -Fe(100) system obtained at +1V for spin down (e) Fe (100)- (borazine)_{n=3} -Fe(100) system obtained at -1V for spin up (f) Fe (100)- (borazine)_{n=4} -Fe(100) system obtained at -1V for spin down, (g) Fe (100)- (borazine)_{n=4} -Fe(100) system obtained at +1V for spin up (h) Fe (100)- (borazine)_{n=4} - Fe(100) system obtained at +1V for spin down.

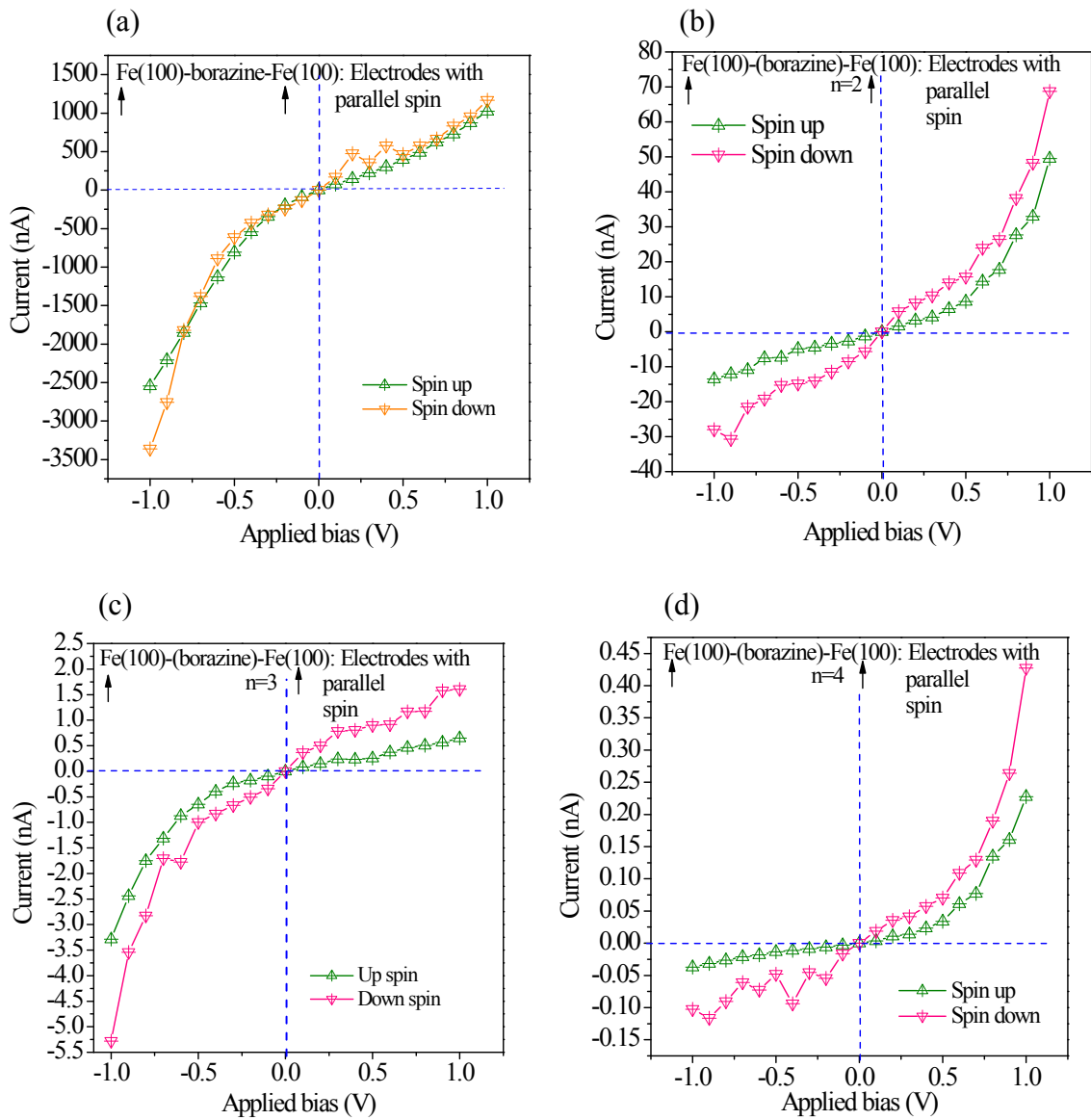


Figure S5. Current (I)- voltage (V) characteristic of (a) Fe(100)-borazine-Fe(100), (b) Fe(100)-(borazine)₂-Fe(100), (c) Fe(100)-(borazine)₃-Fe(100) and (d) Fe(100)-(borazine)₄-Fe(100); under FM arrangement of electrodes.

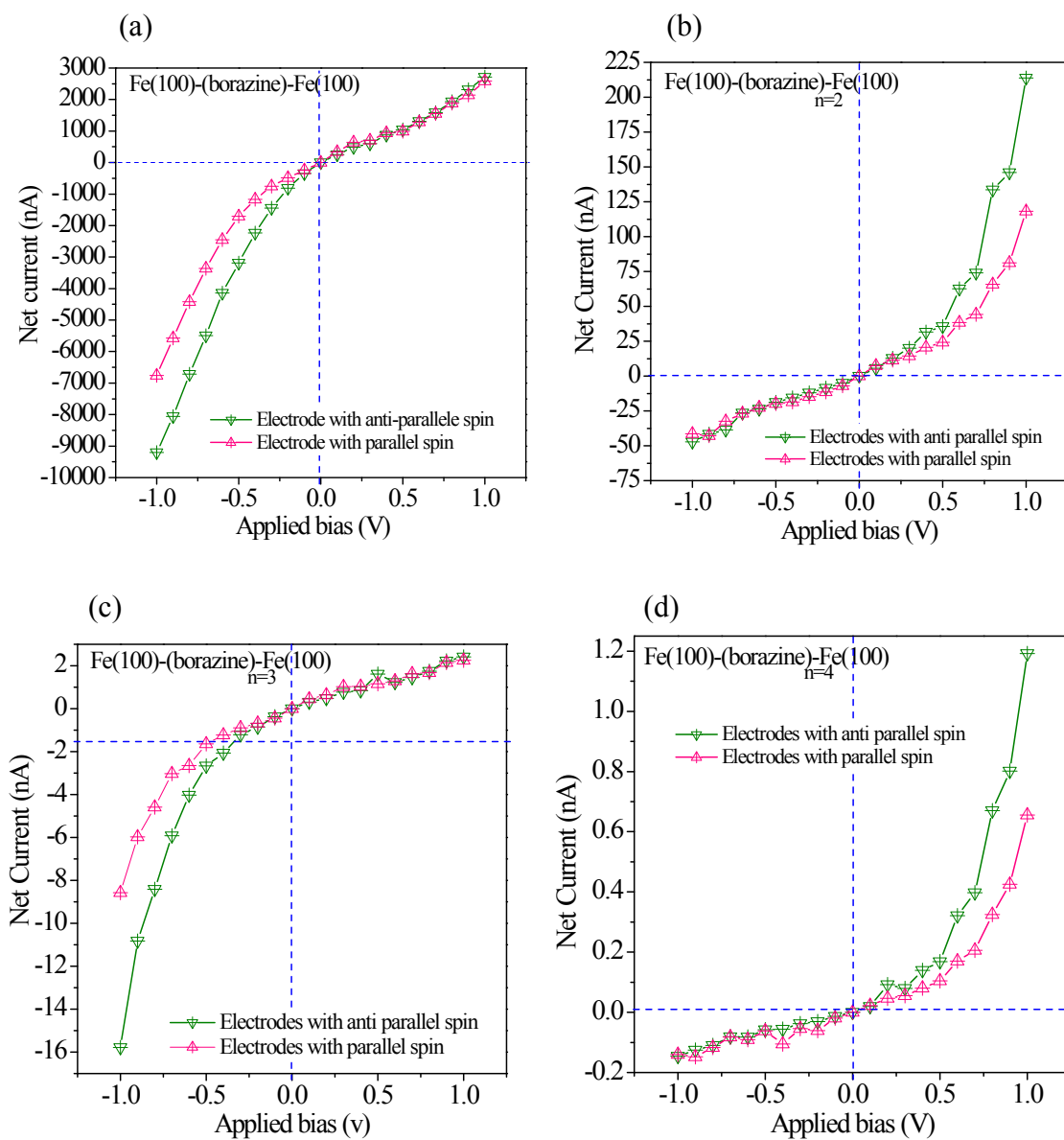


Figure S6: Bias dependence of the net current ($I_{\text{spin up}} + I_{\text{spin down}}$) obtained with spin parallel (FM) and spin anti-parallel (AFM) arrangements of Fe (100) electrodes in case of (a) Fe(100)-borazine -Fe(100), (b) Fe(100)-(borazine)₂-Fe(100), (c) Fe(100)-(borazine)₃-Fe(100) and (d) Fe(100)-(borazine)₄-Fe(100).

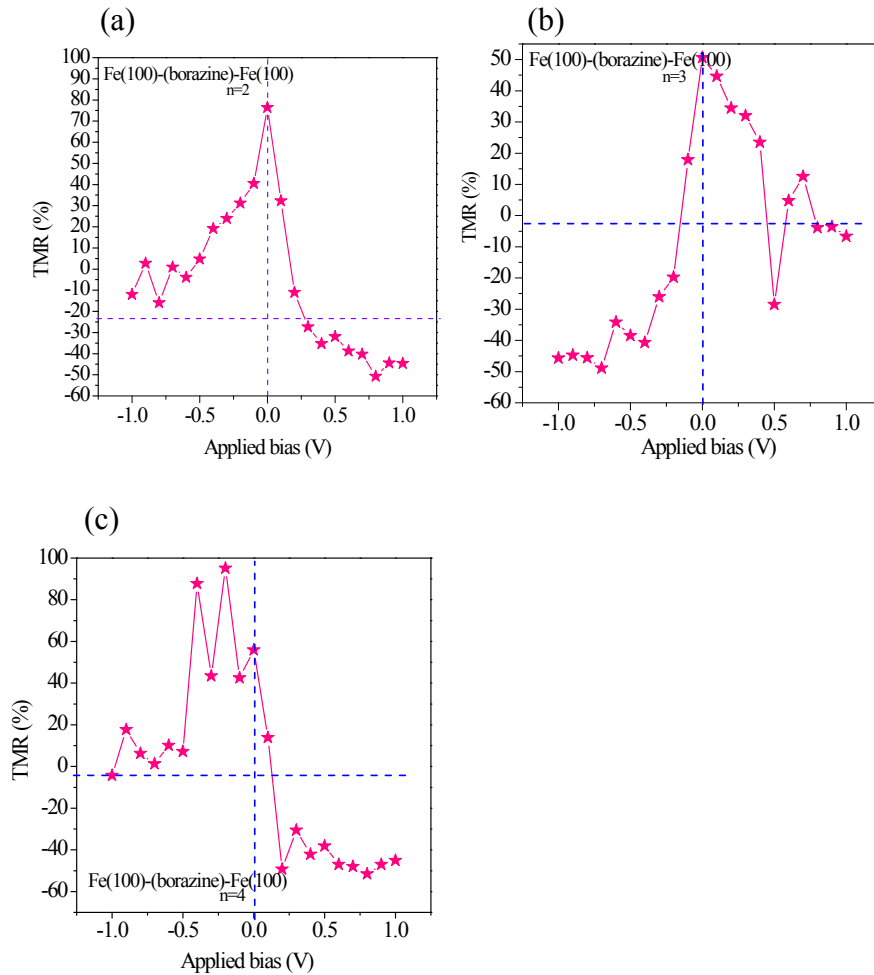
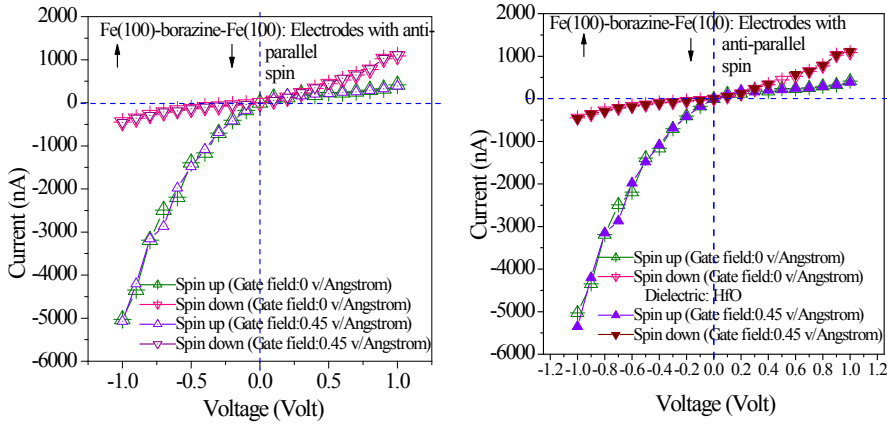


Figure S7. Bias dependence of the TMR of (a) $\text{Fe}(100)\text{-(borazine)}_2\text{-Fe}(100)$, (b) $\text{Fe}(100)\text{-(borazine)}_3\text{-Fe}(100)$ and (c) $\text{Fe}(100)\text{-(borazine)}_4\text{-Fe}(100)$.

Discussion on TMR: The bias dependent variation of tunneling magnetoresistance of the oligomers ($n=2,3$ and 4) are depicted in Figure S6 which clearly suggests that maximum TMR(%) is obtained from the tetramer unit. It is worth commenting that TMR at the molecular break junction could change its sign from positive to negative depending upon the supplied bias and nature of the system and the junction structure of the two-probe set up. The existence of negative TMR has already been verified at the experimental level and justified by theoretical analysis too (Ref 12 and 21 of the main manuscript). The negative TMR has been found in a large number of systems already. Selective references are given below. In our case, we observed significant negative TMR in the forward bias region for the even units of borazine while same feature is observed mostly at the negative bias for odd units. The meticulous inspection of PDOS of the two-probe set up ($n=1$) indicates that the participation

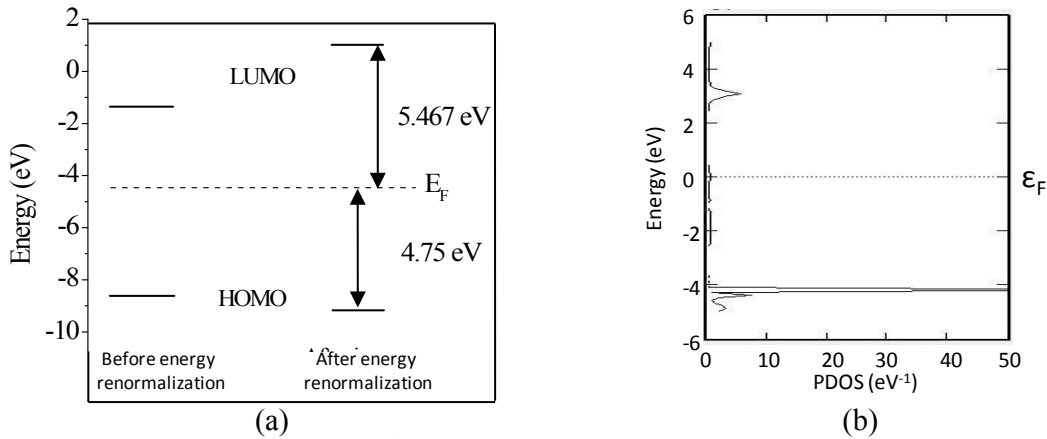
of 3d orbitals of Fe and 3p orbitals of S gets affected with the applied bias which ultimately is responsible for the occurrence of negative TMR in the studied systems.



(a)

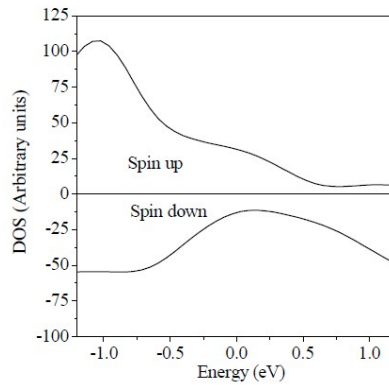
(b)

Figure S8. I-V characteristics of Fe(100)- (borazine)_{n=1}-Fe(100) having the electrodes with spin anti-parallel (AFM) arrangements under variable gate field using two different dielectrics (a) SiO₂ (b) HfO₂



(a)

(b)



(c)

Figure S9: (a) Energy levels of borazine before and after the image potential correction, (b) PDOS of borazine, (c) Partial density of states of Fe 3d electrons. Image charge effect calculation:

In our case, $d=L/2=5.5289 \text{ \AA}$

For small molecule we can assume, $d_0=1 \text{ \AA}$

So According to Souza et. al. (A. M. Souza, I. Rungger, C. D. Pemmaraju, U. Schwingenschloegl, S. Sanvito, Phys. Rev. B. 2013, 88, 165112.) image charge correction,

$$U(d) = -q^2 \ln 2 / 2(d-d_0) = 1.098 \text{ eV}$$

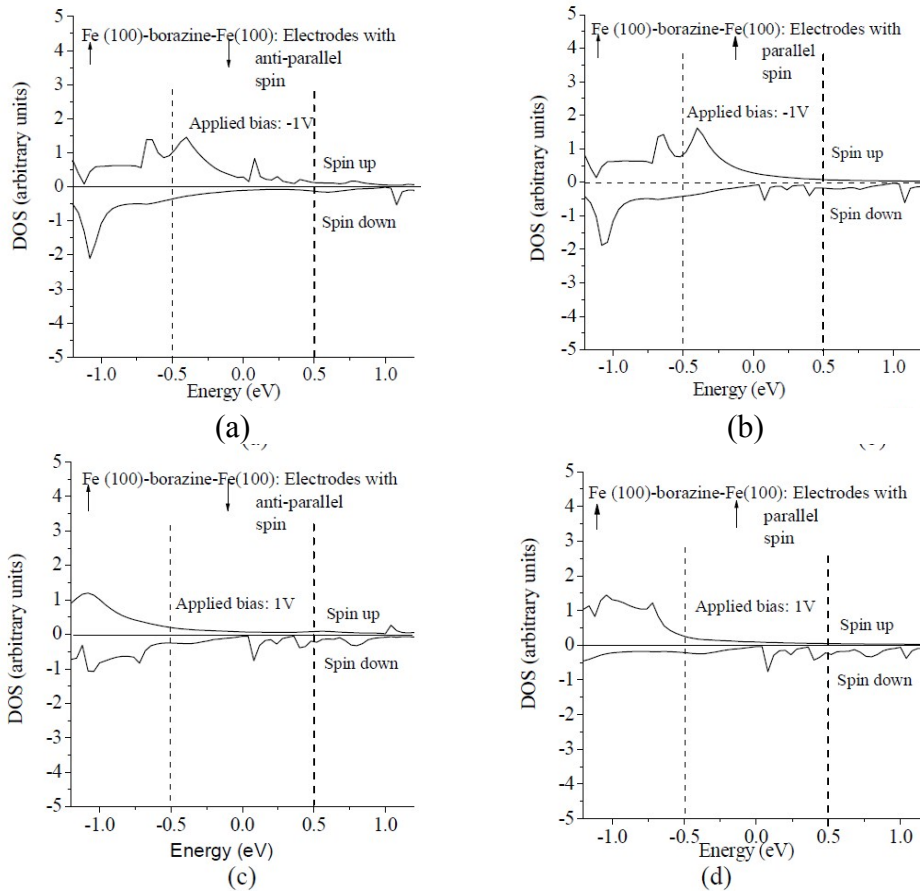


Figure S10. Projected device density of states of 'p' orbitals of sulfur of Fe(100)-borazine-Fe(100) under (a) AFM and (b) FM arrangement of electrodes at -1V potential and (c) AFM and (d) FM arrangement of electrodes at 1V potential.